Fast Reactions of Hydroxycarbenes: Tunneling Effect versus Bimolecular Processes

ARTICLE *in* THE JOURNAL OF PHYSICAL CHEMISTRY A · APRIL 2010

Impact Factor: 2.69 · DOI: 10.1021/jp911655a · Source: PubMed

5 AUTHORS, INCLUDING:

Vitaly G Kiselev
Russian Academy of Sciences
27 PUBLICATIONS **216** CITATIONS
SEE PROFILE

Nguyen Vinh Son
University of Leuven
35 PUBLICATIONS **490** CITATIONS
SEE PROFILE

Nina Gritsan
Russian Academy of Sciences
168 PUBLICATIONS **2,062** CITATIONS
SEE PROFILE

Minh Tho Nguyen
University of Leuven
748 PUBLICATIONS **10,861** CITATIONS
SEE PROFILE

Fast Reactions of Hydroxycarbenes: Tunneling Effect versus Bimolecular Processes

Vitaly G. Kiselev,*,†,‡,§ Saartje Swinnen,† Vinh Son Nguyen,† Nina P. Gritsan,‡,§ and Minh Tho Nguyen*,†

Department of Chemistry, and Mathematical Modeling and Computational Science Center (LMCC), University of Leuven, B-3001 Leuven, Belgium, Institute of Chemical Kinetics and Combustion, 3, Institutskaya Str., Novosibirsk, 630090 Russia, and Novosibirsk State University, 2, Pirogova Str., Novosibirsk, 630090 Russia

Received: December 9, 2009; Revised Manuscript Received: March 7, 2010

Different uni- and bimolecular reactions of hydroxymethylene, an important intermediate in the photochemistry of formaldehyde, as well as its halogenated derivatives (XCOH, X = H, F, Cl, Br), have been considered using high-level CCSD(T)/CBS quantum chemical methods. The Wentzel−Kramers−Brillouin (WKB) and Eckart approximations were applied to estimate the tunneling rate constant of isomerization of *trans*-HCOH to H_2CO, and the WKB procedure was found to perform better in this case. In agreement with recent calculations and experimental observations [Schreiner et al., *Nature* **2008**, *453*, 906], the half-life of HCOH at the low temperature limit in the absence of bimolecular processes was found to be very long (∼2.1 h). The corresponding half-life at room temperature was also noticeable (∼35 min). Bimolecular reactions of *trans*-hydroxymethylene with parent formaldehyde yield primarily more thermodynamically favorable glycolaldehyde via the specific mechanism involving 5-center transition state. The most preferable reaction of *cis*-hydroxymethylene with formaldehyde yields carbon monoxide and methanol. Due to very low activation barriers, both processes occur with nearly a collision rate. If the concentration of HCOH (and its halogenated analogues XCOH as well) is high enough, the bimolecular reactions of this species with itself become important, and H_2CO (or X(H)CO) is then formed with a collision rate. The singlet−triplet energy separation of *trans*-HCOH is confirmed to be ∼−25 kcal/mol.

Introduction

Carbenes, R_1CR_2, form a diverse class of reactive intermediates and play an important role in many areas of chemistry, from combustion to organic synthesis, ligands in metal complexes to photochemistry of aldehydes and ketones.[1,2] The electronic structure and multiplicity of a carbene are strongly dependent on the substituents R_1 and R_2 at the divalent dicoordinated carbon atom, in such a way that electron donor groups tend to stabilize the closed-shell singlet state.[1−3] Although a number of carbenes have been prepared as thermodynamically stable compounds, most of them exist only as short-lived intermediates.[3]

In the present study, we consider the stability and reactivity of some simple hydroxycarbenes (XCOH, X = H, F, Cl, Br, **1**). While methylene (CH_2) has a triplet ground state with a singlet−triplet energy gap of about 9.0 kcal/mol,[4−7] the parent hydroxymethylene (HCOH, **1a**) turns out to have a singlet ground state, with a calculated singlet−triplet separation of −25 kcal/mol.[8−10] In the singlet manifold, hydroxymethylene was calculated to be ∼52 kcal/mol higher in energy than formaldehyde (CH_2O, **2a**),[8] and the unimolecular rearrangement between the two isomers through a 1,2-hydrogen shift is prohibited by an energy barrier of about 28 kcal/mol relative to HCOH.[9−11] In spite of such a relatively large barrier, which implies the existence of HCOH as a detectable species, it had escaped until recent[12] direct spectroscopic detection.

Schreiner et al.[12] applied high-vacuum flash pyrolysis of glyoxylic acid followed by matrix isolation of the products and succeeded in isolating HCOH for the first time. The IR and UV−visible absorption spectra of matrix isolated products have been unambiguously assigned to **1a** with the aid of high-level ab initio quantum chemical calculations. Experiments on the deuterated glyoxylic acid to generate HCOD have also been carried out, and its IR spectrum has been recorded as well.[12] It has been found that a half-life of HCOH is independent of temperature in the range 11−20 K and is equal to ∼2 h. On the contrary, HCOD was found to be stable at the same cryogenic temperatures. These facts give the clear evidence of the tunneling mechanism of **1a** rearrangement to **2a**. High-level quantum chemical calculations[12] also support the proposed mechanism of **1a** decay.

In spite of the low rate constant of the monomolecular rearrangement of **1a**,[12] this species has never been detected at ambient and elevated temperatures. **1a** has been postulated as an intermediate in the photolysis of formaldehyde.[13−18] Its generation has been monitored by ion cyclotron double resonance spectroscopy[19] from which its heat of formation and proton affinity were evaluated. The production of **1a** as a transient species in the reaction of arc generated atomic carbon with water has been proposed on the basis of the rather unusual reactivity observed, and by ab initio calculations as well.[18,20] Formation of HCOH has also been proposed for the pyrolysis of pyruvic acid in the gas phase.[21] Reisler and co-workers[22] studied the photodissociation of CH_2OD radical in the 3s and 3p Rydberg states. From the measured kinetic energy distribution of dissociation products, the heat of formation of the deuterated analogue of hydroxymethylene (HCOD, $\Delta_f H^0 = 24 \pm 2$ kcal/mol) has been determined.[22]

The main goal of the present paper is to consider reactivity of hydroxymethylene and to identify the main reactions leading to its disappearance under diverse conditions. Using quantum

* To whom correspondence should be addressed. E-mails: vitaly.kiselev@kinetics.nsc.ru (V.G.K.), minh.nguyen@chem.kuleuven.be (M.T.N.).
† University of Leuven.
‡ Institute of Chemical Kinetics and Combustion.
§ Novosibirsk State University.

10.1021/jp911655a
Published on Web 04/09/2010

chemical calculations, we have studied a temperature dependence of the rate constant of the **1a** → **2a** transformation occurring by tunneling mechanism. In addition, we have considered different bimolecular reactions of HCOH with formaldehyde as well as processes involving a dimer of **1a** leading to **2a** formation. For the purpose of comparison, the simplest halogenated derivatives XCOH (**1b**−**1d**), with X = F, Cl, and Br, were also considered.

Computational Methods

Electronic structure calculations were carried out using the Gaussian 03 suite[23] of programs. Geometrical parameters of each structure were fully optimized using density functional theory with the B3LYP functional,[24] the quadratic configuration interaction QCISD[25] and the coupled-cluster theory CCSD(T)[26] levels, in conjunction with the correlation consistent aug-cc-pVnZ basis sets with n = D, T, Q.[27] For simplicity, these basis sets are denoted hereafter as aVnZ. Single-point electronic energies were also calculated using the coupled-cluster CCSD(T) formalism in conjunction with the aVnZ basis sets at CCSD(T)/aVTZ optimized geometries for HCOH, and QCISD geometries for halogenated species and dimeric $(XCOH)_2$ forms. Energies of the stationary points on the potential energy surfaces for bimolecular reactions between HCOH and H_2CO were calculated using the CCSD(T)/aVTZ level using the B3LYP/aVTZ optimized geometries.

In the HCOH system, the CCSD(T) energies were extrapolated to the complete basis set (CBS) limit energies using the following expression:[28]

$$E(x) = A_{\mathrm{CBS}} + B\exp(-(x-1)) + C\exp(-(x-1)^2) \tag{1}$$

where $x = 2$, 3, and 4 for the aVnZ basis, n = D, T, and Q, respectively.

The tunneling contributions to the rate constant were estimated using Eckart[29−31] and Wentzel−Kramers−Brillouin (WKB)[32] methods. To obtain the rate constant in the framework of the semiclassical WKB method,[33] one needs to calculate first the barrier penetration integral:

$$\theta(T) = \frac{1}{\hbar}\int_{s_1}^{s_2}\sqrt{2\mu(U(s)-E)}\,\mathrm{d}s \tag{2}$$

where s is the reaction coordinate, $U(s)$ is the potential energy (including the zero-point energy of the normal vibrations orthogonal to a gradient vector), and μ is the corresponding reduced mass. The transmission probability is given by

$$P(E) = \exp(-2\theta(E)) \tag{3}$$

The tunneling rate constant at a fixed energy E is

$$k_{\mathrm{WKB}}(E) = \frac{\omega_0}{2\pi}P(E) = \frac{\omega_0}{2\pi}\exp\left(-\frac{2}{\hbar}\int_{s_1}^{s_2}\sqrt{2\mu(U(s)-E)}\,\mathrm{d}s\right) \tag{4}$$

The physical meaning of this equation is clear: the rate constant is a product of the transmission probability $P(E)$ and the frequency $\omega_0/2\pi$ of the motion in a potential well.

The cross sections of HCOH and HCOD potential energy surfaces for the WKB barrier penetration integral were obtained by intrinsic reaction coordinate (IRC) calculations at the MP2/aVTZ level in mass-weighted Cartesian coordinates with the step 0.1 $\mathrm{amu}^{1/2}$ bohr. The values of energy were then refined using CCSD(T)/aVTZ method and the potential energy curve was fitted with the polynomial expression. The integrals were evaluated numerically.

In the framework of Eckart approach, the cross-section of the potential energy surface along the reaction coordinate is fitted to the energies of three stationary points (zero-point corrected energies of reactant, product and transition state) with the Eckart potential

$$U(x) = \frac{A\exp\left(\frac{x-x_0}{l}\right)}{1+\exp\left(\frac{x-x_0}{l}\right)} + \frac{B\exp\left(\frac{x-x_0}{l}\right)}{\left(1+\exp\left(\frac{x-x_0}{l}\right)\right)^2} \tag{5}$$

The fitting parameters are

$$A = V_{\mathrm{f}} - V_{\mathrm{r}}$$

$$B = (\sqrt{V_{\mathrm{f}}} + \sqrt{V_{\mathrm{r}}})^2$$

$$l = \frac{2\pi}{\omega^*}\sqrt{\frac{2}{\mu}}\left(\frac{1}{\sqrt{V_{\mathrm{f}}}} + \frac{1}{\sqrt{V_{\mathrm{r}}}}\right)^{-1}$$

where V_{f} and V_{r} are the zero-point corrected energy barriers (excluding the vibration corresponding to reaction coordinate) in the forward and reverse direction, ω^* is the absolute value of imaginary frequency of the transition state, and μ is the corresponding reduced mass. The Schrödinger equation can be solved exactly for this type of potential; the transmission probability as a function of energy is

$$P(E) = \frac{\cosh(\alpha+\beta) - \cosh(\alpha-\beta)}{\cosh(\alpha+\beta) + \cosh\delta} \tag{6}$$

where

$$\alpha = \frac{4\pi}{\hbar\omega^*}\left(\frac{1}{\sqrt{V_{\mathrm{f}}}} + \frac{1}{\sqrt{V_{\mathrm{r}}}}\right)^{-1}\sqrt{E}$$

$$\beta = \frac{4\pi}{\hbar\omega^*}\left(\frac{1}{\sqrt{V_{\mathrm{f}}}} + \frac{1}{\sqrt{V_{\mathrm{r}}}}\right)^{-1}\sqrt{E - V_{\mathrm{f}} + V_{\mathrm{r}}}$$

$$\delta = 4\pi\sqrt{\frac{V_{\mathrm{f}}V_{\mathrm{r}}}{(\hbar\omega^*)^2} - \frac{1}{16}}$$

Similarly to (4), the rate constant reads as

$$k_{\mathrm{Eck}}(E) = \frac{\omega_0}{2\pi}P(E) = \frac{\omega_0}{2\pi}\frac{\cosh(\alpha+\beta) - \cosh(\alpha-\beta)}{\cosh(\alpha+\beta) + \cosh\delta} \tag{7}$$

SCHEME 1

H_2+CO ← cis-HCOH (cis-**1a**) ← trans-HCOH (trans-**1a**) → H_2CO (**2a**)

At nonzero temperatures the WKB and Eckart expressions (4) and (7) were averaged over the Boltzmann-populated vibrational levels:

$$k(T) = \frac{\sum_{n=0}^{\infty} k(n\hbar\omega_0) \exp\left(-\frac{n\hbar\omega_0}{kT}\right)}{\sum_{n=0}^{\infty} \exp\left(-\frac{n\hbar\omega_0}{kT}\right)} \quad (8)$$

in which energy is counted from the zero-point vibrational level of the reactant. Actually, only the first two terms in the series expansion contribute to the rate constant noticeably.

Results and Discussion

1. Unimolecular Rearrangement of Hydroxymethylene and Its Halogenated Derivatives XCOH, X = H, F, Cl, and Br. Hydroxymethylene exhibits two conformers, *trans*-**1a** and *cis*-**1a**. The most stable trans-conformer, *trans*-**1a**, has 6.7 kcal/mol lower enthalpy of formation than its cis isomer, *cis*-**1a**.

As mentioned in the Introduction, *trans*-**1a** has singlet ground state that lies well below the triplet counterpart.[8−10] Previous CCSD(T)/CBS calculations made by one of us[8] on *trans*-**1a** led to the values of ΔH_f (*trans*-HCOH) = 26.1 ± 1 kcal/mol for the standard heat of formation at 298 K, and $\Delta E_{ST} = -25.3 \pm 0.5$ kcal/mol for the singlet−triplet gap. Using the focal point analysis, Schreiner and co-workers[12] derived a larger value of −28.0 kcal/mol for ΔE_{ST}. A difference of 2.7 kcal/mol is significant, in view of the fact that both CCSD(T)/CBS used in ref 8 and focal-point analysis in ref 12 are rather similar approaches for high accuracy computations. Having carried out again the CCSD(T)/CBS calculations for the ΔE_{ST} of *trans*-HCOH, we confirmed the results reported earlier.[8] Therefore, we beg to differ with Schreiner et al.[12] on this important thermochemical parameter.

Due to the large singlet−triplet gap, we considered in detail only the reactions of the singlet carbene **1a**. The unimolecular rearrangement of **1a** has already been studied in detail using different quantum chemical procedures.[12,34−36] For the sake of consistency, we discuss hereafter the results obtained at the CCSD(T)/CBS level for all unimolecular reactions of HCOH (Scheme 1). The enthalpy diagram (Figure S1) and geometries of all equilibrium and transition structures under study are presented in the Supporting Information. To compare various levels of theory, we also optimized geometries of all species from Scheme 1 using simpler B3LYP/cc-pVTZ method. A good agreement between both techniques (bond lengths differ less than 0.01 A) was found. On the basis of these results, we used B3LYP/cc-pVTZ geometry optimization in the subsequent calculations (see below).

It is seen from Scheme 1 that two possible channels exist for the disappearance of **1a**, namely, an elimination of H_2 and isomerization to formaldehyde, **2a**. The H_2 elimination from *trans*-**1a** (Scheme 1, left side) is a two-step process. Isomerization to *cis*-**1a** occurs first with an energy barrier of ∼27 kcal/mol (Figure S1, Supporting Information) and the *cis*-**1a** decomposes then to CO and H_2 with a substantial total barrier (51.7 kcal/mol). At the same time, the barrier to isomerization of *trans*-**1a** to **2a** involving transition structure **TS2** (Figure 1)

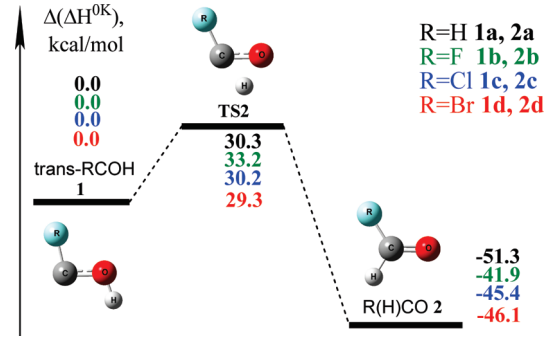

Figure 1. Relative enthalpies at 0 K ($\Delta(\Delta H^{0K})$) of some stationary points on the singlet manifold of H−C−O−H and R−C−O−H (R = F, Cl, Br) systems calculated at CCSD(T)/aVTZ level of theory. The geometry optimization was performed using QCISD/aVDZ method; vibrational frequencies were scaled by a factor of 0.98. *trans*-**1a**−**d** were chosen as reference compounds for the calculations of relative thermodynamic properties. All values are in kcal/mol.

is noticeably lower (30.5 kcal/mol). In agreement with all previous results,[12,34−36] the *trans*-**1a** → **2a** rearrangement is the most important reaction of HCOH disappearance, and we concentrated our efforts on this process.

As opposed to the **1a** case, the reactions of the halogenated derivatives XCOH (**1b**−**1d**, X = F, Cl, Br) have not been considered at a high level of theory, only simple CISD/6-31G(d,p)//HF/4−31G computations have been reported.[37] We calculated the energies of the stationary points on the energy profiles corresponding to halogenated analogues of hydroxymethylene **1b**−**d**. Figure 1 demonstrates that halogenation influences the enthalpy of isomerization and its barrier height insignificantly. The barrier height of **1** → **2** isomerization is ∼30 kcal/mol and does not change significantly for different halogenated derivatives. Due to this fact, the canonical TST rate constant of **1** → **2** reaction is negligible for every halogen substituent R. For instance, the canonical TST rate constant of *trans*-HCOH → H_2CO transformation at 300 K is 4×10^{-10} s^{-1}. If one considers as negligible tunneling contribution to the rate constant, the half-life of **1a** can be estimated as 55 years.

2. Tunneling Contribution to the Rate Constant of HCOH → H_2CO Isomerization. Although the canonical TST rate constant for the **1** → **2** isomerization is too low, the tunneling effect was demonstrated to be very important in the case of *trans*-**1a** → **2a** rearrangement.[12] The authors[12] evaluated the tunneling lifetime of **1a** at 0 K using the WKB approach. In the present work, we determined the *temperature dependence* of the tunneling rate constant using the WKB method and, for the sake of comparison, the profoundly simpler Eckart procedure.

The WKB calculations were made in accordance with formulas (4) and (8) using the polynomial fitted IRC curve and the frequency of the normal mode $\omega_0 = 1210$ cm^{-1} corresponding to the tunneling motion. The results are shown in Figure 2. The zero temperature limit of WKB rate constant ($k = 9.2 \times 10^{-5}$ s^{-1}) corresponds to the half-life $\tau_{1/2} = (\ln 2)/k = 126$ min. This zero temperature value agrees perfectly with the value $\tau_{1/2} = 122$ min obtained earlier by the use of IRC curve calculated at a profoundly higher AE-CCSD(T)/cc-pCVQZ level of theory.[12] The results of matrix isolation experiments[12] are also in good agreement with theoretical predictions. The half-life of *trans*-**1a** varied from 1.7 to 2.0 h in different noble gas matrices in the temperature range 11−20 K.[12] At room temperature (300 K) the calculated half-life of *trans*-**1a** is ∼35 min, which is 3.6 times lower than the zero temperature limit.

The Eckart estimation (6) of the same rate constant was made using the forward and reverse activation barriers (including ZPE

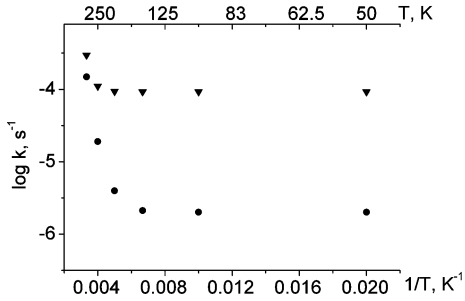

Figure 2. Temperature dependence of WKB (triangles) and Eckart (circles) tunneling rate constants for trans-**1a**→ **2a** rearrangement.

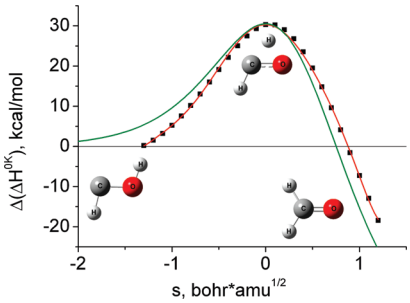

Figure 3. Potential energy profile for the *trans*-**1a** → **2a** transformation along the intrinsic reaction coordinate. Along the IRC (bars), CCSD(T)/aVTZ energies were calculated using MP2/aVTZ geometries; a red curve is the polynomial fitting of IRC points and a green curve is the Eckart fitting of the potential.

without the vibration corresponding to reaction coordinate) $V_f = 32.3$ kcal/mol, $V_r = 84.2$ kcal/mol calculated at the CCSD(T)/CBS level (Figure S1, Supporting Information) and the absolute value of imaginary frequency $\omega^* = 2162$ cm^{-1} for the potential curve fitting. The results are also shown in Figure 2. Note that the discrepancy between Eckart and WKB results is noticeable in a low temperature region, namely, more than an order of magnitude at the zero-temperature limit. However, the rate constants at 250 K agree with each other rather well (Figure 2). The reason of such disagreement at low temperatures is the difference in the shape of potential energy curves (Figure 3).

The behavior of the Eckart potential (5) matched by only three points of potential curve (reactants, products, and transition structure) is not correct at the region of large negative s values; indeed, its tail decreases too slowly. The simple WKB estimation of the transmission probability at low temperatures using formula (3) gives results closer to the exact solution of the Schrödinger equation (6). Due to an incorrect asymptotic behavior of the potential, the absolute value of the barrier penetration integral (2) is overestimated, and thereby the rate constant (4) is underestimated by the order of magnitude at a low temperature limit.

It should also be mentioned that Schreiner et al.[12] found the performance of the Eckart and the WKB procedures to be quantitatively similar in the low temperature limit. Although the barrier values and the PES cross-section were calculated by the authors[12] at a higher level of theory, a good agreement between our barrier values and the WKB low temperature rate constants with earlier results[12] is obtained. Using the parameters of the Eckart model provided in the paper,[12] we obtained the half-life of **1a** $\tau_{1/2} = 25.6$ h at a zero temperature limit. At the same time, using the parameters of Eckart model calculated by us at a CCSD(T)/CBS level, we computed the low temperature half-life $\tau_{1/2} = 95.6$ h. It is also worth mentioning here that the Eckart procedure is very sensitive to small errors in the barrier values (e.g., increasing of the barrier height of the *trans*-**1a** → **2a** reaction by 1 kcal/mol leads to decreasing of the rate constant nearly by 1 order of magnitude). This method suits more for calculation of corrections to TST rate constant at noticeably higher than cryogenic temperatures.

Therefore, only more computationally demanding WKB method yields reasonable results at the low-temperature limit while at room temperature the Eckart approximation also performs well. Because of the large value of the vibrational quantum in *trans*-**1a** (1210 cm^{-1}), only the first two terms in eq 8 are significant (even at 300 K the population of the first vibrational level $v = 1$ is 0.3%). At the same time, this is the reason for the relatively high temperature (about 200 K) of the transition from the dominant ground state to thermally activated tunneling.

The tunneling rate constant for HCOD, the isotope analogue of **1a**, was found to be negligible (WKB low temperature lifetime is more than 30 years). This fact also agrees well with the experimental data and previous computations.[12]

3. Bimolecular Reactions of HCOH with H_2CO. Although the unimolecular reactions of **1a** are rather slow, **1a** had escaped experimental detection at ambient and elevated temperatures. The bimolecular reactions, especially at higher pressure and in the condensed phase, may be responsible for the disappearance of **1a**. As mentioned in the Introduction, **1a** was proposed as a key intermediate in the photochemistry of formaldehyde, **2a**.[10,14−16,38] Let us note that photolysis of **2a** in an argon matrix at low dilution (1:40)[14] yields glycolaldehyde (**3a**), methanol, and carbon monoxide as the detected products. In subsequent theoretical papers,[17,18] a series of bimolecular reactions of **1a** and **2a** leading to the detected products were proposed. However, calculations were performed at the rather low levels (HF and MP2 with small basis sets) typical of the 1980s. In the present work, we applied the highly accurate quantum chemical techniques for the study of bimolecular reactions of **1a**.

It was found that both *trans*-**1a** and *cis*-**1a** form quite stable H-bonded complexes with formaldehyde **2a** (Figure 4 and 5, complexes **C1a** and **C2a**, correspondingly). The enthalpy of formation of these complexes was estimated to be 6.6 and 8.9 kcal/mol for *cis*- and *trans*-**1a**, respectively. Therefore, bimolecular reactions of **1a** and **2a** should proceed through these complexes.

It is well documented[2] that C−H insertion and double bond addition are typical of singlet carbenes. However, McKee et al.[18] pointed out that another reaction, specific particularly for *trans*-**1a** and formaldehyde **2a**, might proceed via a 5-center transition structure (Figures 4 and 5, cf. $\mathbf{TS_{C1}}$). The barrier of this reaction is very low (∼1 kcal/mol), mostly due to very early transition state, which in turn is due to the high exothermicity of the process (∼−65 kcal/mol). The barrier of C−H insertion ($\mathbf{TS_{C2}}$, Figure 4 and 5) was found to be much higher (∼5 kcal/mol). However, for the particular *trans*-**1a** + **2a** system, both reactions lead to the same product: glycolaldehyde **3a**. The barrier of another possible competing process, namely the C═O addition, leading to formation of hydroxyoxirane **4a** via transition structure $\mathbf{TS_{C3}}$ (Figure 4 and 5) is remarkably larger (∼20 kcal/mol).

Attempts to estimate the barrier of C−H insertion have been previously made at the Hartree−Fock level (the authors were not able to localize the transition state)[17] and second-order perturbation theory MP2 ($\mathbf{TS_{C2}}$ lay 9.7 kcal/mol above the separated *trans*-**1a** + **2a**)[18] levels, and using multilevel G2M procedure ($\mathbf{TS_{C2}}$ lay 37.9 kcal/mol above the *trans*-**1a** + **2a** asymptote)[39] as well. Our value of barrier height turns out to be tremendously lower (−3.7 kcal/mol below the *trans*-**1a** +

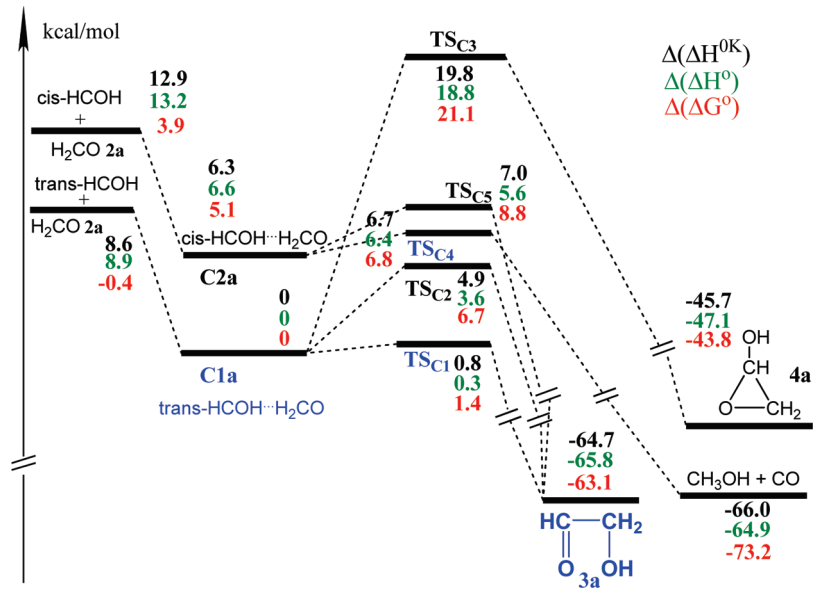

Figure 4. The relative enthalpies at 0 K ($\Delta(\Delta H^{0K})$), the relative enthalpies ($\Delta(\Delta H^{0})$), and Gibbs free energies ($\Delta(\Delta G^{0})$) at 298 K of stationary points corresponding to the bimolecular reactions of **1a** with **2a**. Calculations were performed at CCSD(T)/aVTZ//B3LYP/cc-pVTZ level of theory; vibrational frequencies were scaled by a factor 0.985. The complex of *trans*-**1a** with **2a** (**C1a**) was chosen as a reference for relative thermodynamic properties. All values are given in kcal/mol.

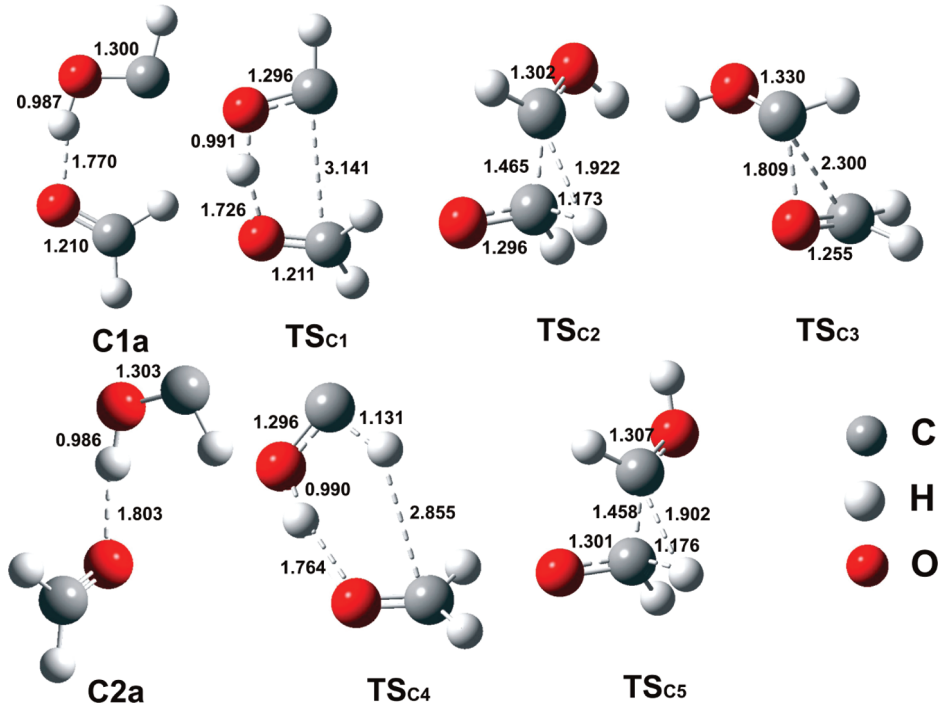

Figure 5. Bond lengths (in Å) in different complexes of **1a** and **2** and transition structures of their reactions optimized at the B3LYP/cc-pVTZ level.

2a, Figure 4) than the ones calculated before. The possible source of discrepancy in this case might be an insufficient performance of employed earlier MP2 procedure with small basis sets.[18,39]

The 5-center transition state of another competing process (**TS$_{C1}$**, Figure 4 and 5) was found to lie ~1 kcal/mol below the complex **C1a**.[18] This result was indeed due to separate geometry optimization at a HF level and a subsequent refinement of the energy value using single point MP2 procedure.[18] Higher level of theory yields in this case a reasonable value of 0.8 kcal/mol (Figure 4).

Thus, one may conclude that reactions of *trans*-**1a** with **2a** lead exclusively to formation of **3a**. The most favorable process proceeds with very low barrier through the specific 5-center transition state (**TS$_{C1}$**). Though the energy barrier of C−H insertion (**TS$_{C2}$**) was calculated to be significantly lower than it was proposed earlier,[17,18,39] this process is still less favorable than the one proceeding via **TS$_{C1}$**. The C═O addition does not play an important role in this case. Taking into account the fact that the energy barrier of the reaction proceeding via **TS$_{C1}$** (Figure 4) is very low (~1 kcal/mol), and the only competing C−H insertion reaction (**TS$_{C2}$**, Figure 4 and 5) leads to the same product **3a**, formation of **3a** is expected to occur at room and elevated temperatures with nearly a collision rate constant.

In the case of *cis*-**1a**, the 5-center transition structure is no longer possible due to geometric constraints. At the same time,

another reaction can proceed via transition structure $\mathbf{TS_{C4}}$ (Figure 4 and 5), which is a simultaneous transfer of two H atoms to O- and CH_2-moieties of **2a** yielding CH_3OH and CO. This process is also highly exothermic (∼−65 kcal/mol) and the energy barrier is very low, being ∼0.4 kcal/mol. The C−H insertion yielding **3a** is slightly less favorable (the Gibbs energy of activation being ∼2 kcal/mol). Similar to the reactions of *trans*-**1a**, the barrier to C═O addition is high and this process is not important for the mechanism of *cis*-**1a** disappearance. Therefore, *cis*-**1a** reacts with formaldehyde at ambient and elevated temperatures with a collision rate constant yielding CH_3OH and CO.

If the equilibrium between *cis*- and *trans*-**1a** is taken into account ($\Delta(\Delta G^0) = 6.7$ kcal/mol at CCSD(T)/CBS), the yield of CH_3OH + CO formed in reaction of *cis*-**1a** and **2a** via $\mathbf{TS_{C4}}$ is about 10^5 times lower at room temperature than the yield of **3a** formed in the reaction of *trans*-**1a** and **2a** via $\mathbf{TS_{C5}}$.

Note that *trans*-**1a** and *cis*-**1a** form with **2a** stable H-bonded complexes **C1a** and **C2a**. The barriers to subsequent reactions through transition structures $\mathbf{TS_{C1}}$ and $\mathbf{TS_{C4}}$ (Figure 4) are very low. These transition structures lie well below the corresponding asymptotes [*trans*-**1a** + **2a**] and [*cis*-**1a** + **2a**] (Figure 4). It is therefore reasonable to expect that the bimolecular reactions of **1a** with **2a** in the gas phase will occur with small negative activation energy yielding presumably glycolaldehyde **3a**.

Theoretical predictions agree well with the results of photolysis of **2a** in an argon matrix at low dilution.[14] The latter authors detected **3a**, methanol, and carbon monoxide among the products. Formation of **3a** might therefore be attributed to the reaction of *trans*-**1a** with **2a** via $\mathbf{TS_{C1}}$ and CH_3OH and CO are formed in the reaction of *cis*-**1a** with **2a** via $\mathbf{TS_{C4}}$. Note that reactions can proceed at cryogenic temperature (12 K) only if their barriers do not exceed ∼1 kcal/mol. This fact agrees quantitatively with the computed values of activation barriers corresponding to the transition states $\mathbf{TS_{C1}}$ and $\mathbf{TS_{C4}}$ (Figure 4).

At very low concentrations of H_2CO, the unimolecular (tunneling) reaction **1a** → **2a** becomes faster than the bimolecular processes. Assuming the bimolecular reactions to occur with a collision rate constant and the WKB rate constant of unimolecular reaction to be 10^{-4} s^{-1} at room temperature (see above), the corresponding concentration of H_2CO is estimated to be very low, being about 10^6 cm^{-3}. The unimolecular reaction thus dominates at the pressures below this value.

4. Conversion of XCOH in the H-Bonded Dimers. As shown above, reactions of **1a** with **2a** are likely to be responsible for the fast disappearance of **1a** generated upon photolysis of formaldehyde. However, if the concentration of **1a** is sufficiently high, other reactions might also become important. For instance, **1a** and its halogenated analogues **1b**−**1d** could form hydrogen-bonded dimers in the gas phase at ambient and even elevated temperatures. Figure 6 displays the structures of H-bonded dimers of *trans*-**1b**−**1d** (**D1b**−**D1d**). The enthalpy of formation of such dimers is quite large, being ∼−20 kcal/mol. We were not able to optimize the dimer structure **D1a** at the QCISD/aVDZ level. It was also not possible to locate the **D1a** structure at the HF, MP2, and B3LYP levels. All attempts invariably led to the markedly more favorable dimer of formaldehyde molecules **D2a**.

Figure 6 shows that a concerted double hydrogen atom transfer in the H-bonded dimers of hydroxymethylenes, **D1b**−**d**, leads to the dimers of corresponding substituted formaldehydes **D2b**−**d**. The barriers on the PES between two type of dimers (**D1b**−**d** and **D2b**−**d**, transition structure $\mathbf{TS_{D2}}$) are extremely

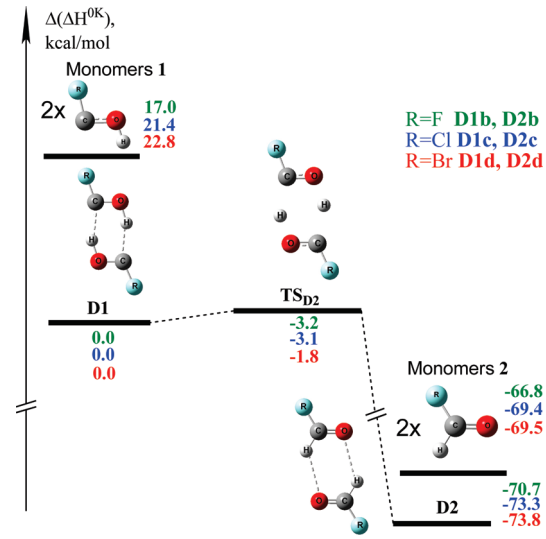

Figure 6. Relative enthalpies of the H-bonded dimers of halogenated derivatives of hydroxymethylenes (**D1b**−**D1d**) and formaldehydes (**D2b**−**D2d**) calculated at CCSD(T)/aVTZ level of theory. The geometry optimization and vibrational frequency calculations were performed at the QCISD/aVDZ level, vibrational frequencies were scaled by the factor 0.98. The dimers **D1b**−**D1d** were chosen as reference for relative thermodynamic properties. All values are in kcal/mol.

small, in such a way that when the zero-point energy is taken into account, energies of the transition structures drop below the corresponding **D1b**−**d**. A possible reason for such a slightly negative barrier heights is the use of different levels of theory for geometry optimization and subsequent single-point energy refinement. Whatever the case, it is clear that the transformation of the initial **1b**−**1d** complexes to the **2b**−**2d** products, respectively, occurs with nearly a collision rate constant.

Conclusion

On the basis of our calculations, the following remarks on the reactivity of the singlet hydroxymethylene, HCOH, and its halogenated derivatives can be made. First, although the high energy barrier of unimolecular reaction HCOH → H_2CO makes this reaction classically prohibited, the contribution of tunneling is very significant in this case. Two different procedures, viz., WKB and Eckart approximations, were applied to evaluate the tunneling rate constant, and only the WKB procedure was found to perform well. The half-life of HCOH at room temperature in the absence of bimolecular processes was found to be long (∼35 min). As HCOH is a possible component in interstellar matter,[40−42] this unimolecular process might be responsible for its depletion.

In the bimolecular reactions of hydroxymethylene with the formaldehyde, the complex of *trans*-hydroxymethylene with formaldehyde is prone to a fast transformation giving the more thermodynamically favorable glycolaldehyde via a mechanism involving a 5-center transition structure. The most preferable reaction of *cis*-hydroxymethylene with formaldehyde yields carbon monoxide and methanol. Due to very low activation energies, both processes occur with nearly a collision rate. If the concentration of HCOH (and its halogenated analogues XCOH as well) is high enough, the bimolecular reactions of these species with itself become predominant. In such situation, the hydroxycarbene turns out to be extremely unstable, and the formaldehyde isomer H_2CO (X(H)CO) is formed with a collision rate.

Finally, we confirmed the previous result[8] that singlet−triplet energy separation of *trans*-HCOH amounts to ∼−25 kcal/mol.

Acknowledgment. The Leuven group is indebted to the KULeuven Research Council (GOA, IUAP programs) for continuing support. V.G.K. also appreciates the support of this work by the Russian Federal Agency of Education (project NK-187P(6), contract P1475), INTAS (project YSF 06-1000014-6324), and SB RAS (Lavrentiev grant program). V.G.K. is thankful to Prof. Alexey V. Baklanov for very useful discussions.

Supporting Information Available: Cartesian coordinates of all compounds under study (txt file). Stationary points on the PES for HCOH transformations (Figure S1, pdf file). This material is available free of charge via the Internet at http://pubs.acs.org.

References and Notes

(1) Bertrand, G. *Carbene Chemistry*; Marcel Dekker: New York, 2002.
(2) Moss, R. A.; Platz, M. S.;, Jr. *Reactive Intermediate Chemistry*; Wiley Interscience: Hoboken, NJ, 2004.
(3) Bourissou, D.; Guerret, O.; Gabbai, F. P.; Bertrand, G. *Chem. Rev.* **2000**, *100*, 39.
(4) Feller, D.; Dixon, D. A. *J. Phys. Chem. A* **2000**, *104*, 3048.
(5) Ruscic, B.; Litorja, M.; Asher, R. L. *J. Phys. Chem. A* **1999**, *103*, 8625.
(6) Hu, C. H. *Chem. Phys. Lett.* **1999**, *309*, 81.
(7) Leopold, D. G.; Murray, K. K.; Lineberger, W. C. *J. Chem. Phys.* **1985**, *83*, 4849.
(8) Matus, M. H.; Nguyen, M. T.; Dixon, D. A. *J. Phys. Chem. A* **2006**, *110*, 8864.
(9) Harding, L. B.; Schelegel, H. B.; Krishnan, R.; Pople, J. A. *J. Phys. Chem.* **1980**, *84*, 3394.
(10) Goddard, J. D.; Schaefer, H. F. *J. Phys. Chem.* **1979**, *70*, 5117.
(11) Pople, J. A.; Raghavachari, K.; Frisch, M. J.; Binkley, J. S.; Schleyer, P. V. *J. Am. Chem. Soc.* **1983**, *105*, 6389.
(12) Schreiner, P. R.; Reisenauer, H. P.; Pickard IV, F. C.; Simmonett, A. C.; Allen, W. D.; Matyus, E.; Csaszar, A. G. *Nature* **2008**, *453*, 906.
(13) Houston, P. L.; Moore, C. B. *J. Chem. Phys.* **1976**, *65*, 757.
(14) Sodeau, J. R.; Lee, E. K. C. *Chem. Phys. Lett.* **1978**, *57*, 71.
(15) Lucchese, R. R.; Schaefer, H. F. *J. Am. Chem. Soc.* **1978**, *100*, 298.
(16) Kemper, M. J. H.; van Dijk, J. M. F.; Buck, H. M. *J. Am. Chem. Soc.* **1978**, *100*, 7841.
(17) Kemper, M. J.; Hoeks, C. H.; Buck, H. M. *J. Chem. Phys.* **1981**, *74*, 5744.
(18) Ahmed, S. N.; McKee, M. L.; Shelvin, P. B. *J. Am. Chem. Soc.* **1985**, *107*, 1320.
(19) Pau, C. F.; Hehre, W. J. *J. Phys. Chem.* **1982**, *86*, 1252.
(20) Ahmed, S. N.; McKee, M. L.; Shelvin, P. B. *J. Am. Chem. Soc.* **1983**, *105*, 3942.
(21) Weiner, B. R.; Rosenfeld, R. N. *J. Org. Chem.* **1983**, *48*, 5362.
(22) Feng, L.; Demyanenko, A.; Reisler, H. *J. Chem. Phys.* **2004**, *120*, 6524.
(23) Frisch, M. J.; Trucks, G. W.; Schlegel, H. B.; Scuseria, G. E.; Robb, M. A.; Cheeseman, J. R.; Montgomery, J. A., Jr.; Vreven, T.; Kudin, K. N.; Burant, J. C.; Millam, J. M.; Iyengar, S. S.; Tomasi, J.; Barone, V.; Mennucci, B.; Cossi, M.; Scalmani, G.; Rega, N.; Petersson, G. A.; Nakatsuji, H.; Hada, M.; Ehara, M.; Toyota, K.; Fukuda, R.; Hasegawa, J.; Ishida, M.; Nakajima, T.; Honda, Y.; Kitao, O.; Nakai, H.; Klene, M.; Li, X.; Knox, J. E.; Hratchian, H. P.; Cross, J. B.; Bakken, V.; Adamo, C.; Jaramillo, J.; Gomperts, R.; Stratmann, R. E.; Yazyev, O.; Austin, A. J.; Cammi, R.; Pomelli, C.; Ochterski, J. W.; Ayala, P. Y.; Morokuma, K.; Voth, G. A.; Salvador, P.; Dannenberg, J. J.; Zakrzewski, V. G.; Dapprich, S.; Daniels, A. D.; Strain, M. C.; Farkas, O.; Malick, D. K.; Rabuck, A. D.; Raghavachari, K.; Foresman, J. B.; Ortiz, J. V.; Cui, Q.; Baboul, A. G.; Clifford, S.; Cioslowski, J.; Stefanov, B. B.; Liu, G.; Liashenko, A.; Piskorz, P.; Komaromi, I.; Martin, R. L.; Fox, D. J.; Keith, T.; Al-Laham, M. A.; Peng, C. Y.; Nanayakkara, A.; Challacombe, M.; Gill, P. M. W.; Johnson, B.; Chen, W.; Wong, M. W.; Gonzalez, C.; Pople, J. A. *Gaussian 03*, Revision E.01; Gaussian, Inc.: Wallingford, CT, 2004.
(24) Becke, A. D. *J. Chem. Phys.* **1993**, *98*, 5648.
(25) Pople, J. A.; Head-Gordon, M.; Raghavachari, K. *J. Chem. Phys.* **1987**, *87*, 5968.
(26) Raghavachari, K.; Trucks, G. W.; Pople, J. A.; Head-Gordon, M. *Chem. Phys. Lett.* **1989**, *157*, 479.
(27) Dunning, T. H. *J. Chem. Phys.* **1989**, *90*, 1007.
(28) Peterson, K. A.; Woon, D. E.; Dunning, T. H. *J. Chem. Phys.* **1994**, *100*, 7410.
(29) Eckart, C. *Phys. Rev.* **1930**, *35*, 1303.
(30) Johnston, H. S.; Heicklen, J. *J. Phys. Chem.* **1962**, *66*, 532.
(31) Truong, T. N.; Truhlar, D. G. *J. Chem. Phys.* **1990**, *93*, 1761.
(32) Landau, L. D.; Lifshits, E. M. *Quantum mechanics*; Pergamon Press: New York, 1965.
(33) Skodje, R. T.; Truhlar, D. G.; Garrett, B. C. *J. Phys. Chem.* **1981**, *85*, 3019.
(34) Zhang, X.; Zou, S.; Harding, L.; Bowman, J. *J. Phys. Chem. A* **2004**, *108*, 8980.
(35) Koziol, L.; Mozhayskiy, V.; Braams, B.; Bowman, J.; Krylov, A. *J. Phys. Chem. A* **2009**, *113*, 7802.
(36) Koziol, L.; Wang, Y.; Braams, B. J.; Bowman, J. M.; Krylov, A. I. *J. Chem. Phys.* **2008**, *128*, 204310.
(37) Morokuma, K.; Kato, S.; Hirao, K. *J. Chem. Phys.* **1980**, *72*, 6800.
(38) Reid, D. L.; Hernandez-Trujillo, J.; Warkentin, J. *J. Phys. Chem. A* **2000**, *104*, 3398.
(39) Leon, S. *Chem. Phys. Lett.* **1998**, *296*, 292.
(40) Green, S.; Herbst, E. *Astrophys. J.* **1979**, *229*, 121.
(41) Hoffman, M. R.; Schaefer, H. F., III. *Astrophys. J.* **1981**, *249*, 563.
(42) Ohishi, M.; Ishikawa, S.; Amano, T.; Oka, H.; Irvine, W. M.; Dickens, J. E. *Astrophys. J. Lett.* **1996**, *471*, L61.

JP911655A